The 2009 IEEE/RSJ International Conference on
Intelligent Robots and Systems
October 11-15, 2009 St. Louis, USA

Vehicle 3*D* Localization in Mountainous Woodland Environments.

Yoichi MORALES, Takashi TSUBOUCHI and Shin'ichi YUTA

Abstract— **This paper presents an approach for vehicle 3*D* localization in outdoor woodland environments using a loosely coupled multisensor system. The vehicle 3*D* dead reckoning is computed using a wheel encoder and an IMU. Dead reckoning is corrected from three different sources: a)Using a tilted lidar for road detection and computation of the vehicle position within the road which is then corrected towards a 2*D* road centerline map given in advance. b) DGPS 2*D* or 3*D* data as available. c) Under tree foliage DGPS blackouts commonly occur, specially when measuring height, therefore the use of a barometer for correcting height is proposed. An extended Kalman filter is used for sensor fusion and pose estimation. Finally, the estimated vehicle height is added to the 2*D* map obtaining a 3*D* road centerline map with width (measured by the tilted lidar). Thoroughly experimentation on real mountainous woodland paths show the usefulness and robustness of the proposed approach.**

I. Introduction

A. Research Motivation

The motivation of this research is the automation of construction machines. The particular problem of interest is a dump truck navigating in forested paths situated in mountainous environments where a previously constructed map is available. In order to achieve autonomous navigation in a map-based approach, vehicle localization is crucial. This research objective is the development of a robust and reliable localization system for outdoor mountainous forested paths. In this research, a mountainous forested path is defined as a path with ups and downs where a wheeled vehicle can traverse. The road has some open areas but is mostly surrounded by trees.

Vehicle localization is the process of determining and tracking the position (location) of a vehicle relative to its environment. Outdoor vehicle localization is a challenging field that still have unexplored areas open for research. There are many factors that make outdoor vehicle position estimation difficult such as cluttered environments where there are illumination, weather, and vegetation changes. In outdoor environments, common odometry fails because of non-flat irregular surfaces, dead reckoning based on inertial units is subject to integration errors. In mountainous environments where there are ups and downs, vehicle 3D localization is necessary. If a map containing 3D data is available, the correct estimation of vehicle's height could create hypotheses of robot's position even if the initial conditions are not known. The problem of such approach is the unavailability of accurate 3D maps in woodland environments. Maps created with satellite photographs and lidars on helicopters or airplanes can not distinguish accurately roads under tree foliage. On the other hand, GPS is not reliable when there are tall obstacles around. There are some 3D maps available which have a resolution of tens of meters which would not be suitable for vehicle localization purposes.

The contributions of this paper are threefold. The first is the vehicle 6*DoF* localization using dead reckoning corrected towards a road centerline map and corrected by DGPS when available. The second is the height correction using a barometer when DGPS is not available. The third is the extension of available 2*D* road centerline maps to 3*D* maps with the road width added as a parameter.

The outline of the rest of the paper is as follows: Section II presents related works, Section III describes the hardware, Section IV details the localization approach and finally Sections V and VI presents the experiments and conclusions.

II. Related Works

For vehicle localization landmarks are commonly used for vehicle localization. In [1] the use of natural and artificial landmarks for vehicle localization is treated in a SLAM approach. The problems of use of artificial landmarks for large scale environments is that it is a time and effort consuming approach. On the other hand, the use of natural features as landmarks such as trees has being proposed in [2] and [3]. In [4] a SLAM system for forest harvesters use tree trunks as features; in this work, it is mentioned that tree trunk extraction in dense forests is a difficult difficult task if not impossible. In [5] mapping of vast environments with trees is treated where tree trunks are modeled as cylinders. The use of tree trunks as landmarks is restricted by the type of trees and vegetation around them (which could occlude trees and change its characteristics depending of the season of the year). The use of roads for vehicle localization has been proposed in [6] in a SLAM approach where the road curbs were extracted, in this work, roads with and without curbs are also extracted. An approach for vehicle localization in outdoor environments without the need for GPS using multilevel surface maps with active sensing has being proposed in [7] where the vehicle uses multiple hypothesis to localize itself within the map. The disadvantage of this approach is that for large scale environments (several kilometers), the map building would be computer memory demanding and time and effort consuming. In this work the vehicle corrects its position towards the road centerline

This work has been supported by the Japan Society of Promotion of Science (JSPS) Grant-in-Aid for Scientific Research (Scientific Research (B)) under contact number 18360116

Y. Morales, T. Tsubouchi and S. Yuta are with Graduate School of Systems and Information Engineering University of Tsukuba, Tsukuba, 305-8573, Japan (yoichi,tsubo,yuta)@roboken.esys.tsukuba.ac.jp

in a map matching approach. A similar work was done by M. Najjar in [8] who presented an approach using a Kalman filter for vehicle localization and belief theory for road selection. Najjar defined the map observation as the orthogonal projection of the estimated position to the road line segment. In this work a lidar is used to precisely measure the position of the vehicle towards the road center, where the covariance of the observation is given by the dispersion of the scan points when detecting the centerline. The road the vehicle followed was pre-selected from a road network, therefore the road segment selection is out of the issues of this work.

DARPA Grand and Urban challenges proved that the present state of the art is enough to achieve long range autonomous navigation. Urmson et al., in [9] used Applanix POS-LV 220/420 GPS/IMU system. A filter was used to estimate the displacement between the solution of the POS-LV sensor and the road boundaries detected to keep the vehicle localization smooth even when jumps caused by GPS were present. Montemerlo et al., in [10] used the Applanix POS-LV for vehicle localization where a filter was designed to keep smooth the position estimation by the POS-LV sensor and the road lines or curbs detected by the laser scanners. Bacha et al., in [11] used NovAtel's ProPak-LB+ GPS/INS system coupled with wheel speed and angle measurements available from the vehicle interface with an extended Kalman filter for localization. Bohren et al., in [12] used an Oxford Technical Solutions RT3050 Inertial and GPS Navigation System combined with wheel odometry. Leonard et al., in [13] used the Applanix POS-LV 220 GPS/INS system to estimate the vehicle position. Miller et al., in [14] developed its own tightly-coupled localization system using an extended square root information filter composed of four sensors: the ABS wheel encoders, an IMU, one three antenna GPS receiver which outputs raw data an a single antenna GPS receiver. The common factor within all the previous approaches is that all of them use GPS/INS systems with odometry and as these systems by themselves can not provide position accurate and reliable enough all the time they have to be assisted by corrections towards a road map. The main difference of this work towards the previous works is the environment where the system was experimentally tested. The practical contribution is the report of experimental results held in large mountainous woodland paths.

This paper reports a loosely coupled system approach for 6DoF vehicle localization in forested outdoor environments where GPS blackouts often occur. A previously selected 2D road centerline map is given in advance. The road segment selection is out of the issues of this work.

III. Hardware System

The hardware used for vehicle localization is composed of a wheel encoder (CORRSYS-DATRON wheel pulse transducer), an IMU (Crossbow NAV420CA) and a DGPS receiver (Trimble DSM12/212). A lidar tilted 29^o (Hokuyo Top-URG) for road extraction and a barometer (Druck DPI740) complement the system. All sensors were attached to a Mitsubishi Delica van. The sensors are connected to a Panasonic TOUGHBOOK CF-30 with a 1.66Gz Intel core duo processor, installed with ubuntu 8.04 Linux (kernel 2.6.24-19). The purpose of having multi sensors is to have a redundant system. In a system with hardware redundancy (sensor redundancy), a variable can be measured in more than one way, offering the possibility of covering the lack of availability of one sensor with another.

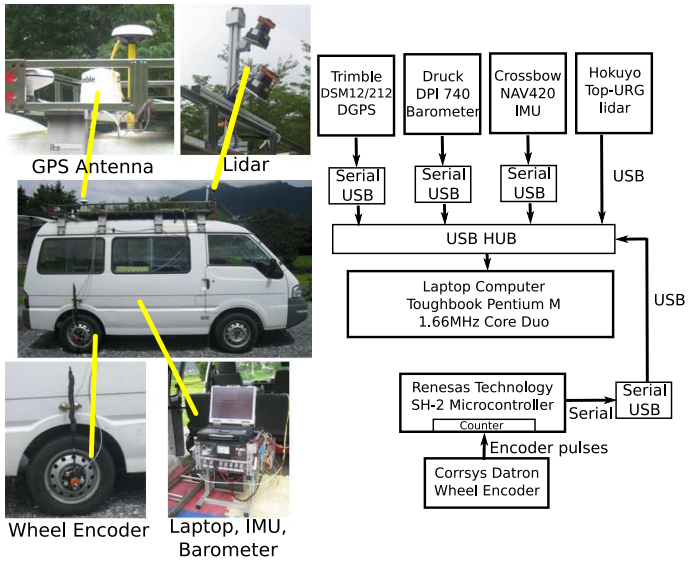

Fig. 1: Wheel encoder, GPS, IMU, lidar, barometer and laptop attached to the experimental vehicle. Sensors connected to a laptop through USB.

Use of a Barometer for Height Computation EXPERIMENTS SHOULD BE MORE CLEAR

The barometric sensor used in this work measures the atmospheric pressure with a precision of $\pm 0.15mbar$. It outputs height above sea level in meters in text mode via RS232C port with a rate of $1Hz$. The relation between static pressure and pressure altitude [1] up to $11000m$ can be expressed as:

$$z = (1 - ((P/Po)^{0.190263}))288.15/0.00198122, \qquad (1)$$

where Po is the pressure at mean sea level ($1013.25hPa$) and P is the atmospheric static pressure at the placed height. According to the previous formula and if temperature is constant, DPI740 sensor has a height precision of $1.2487m$. In the real world, the atmospheric static pressure and the temperature are not constant, this causes variations in measured height of several tens of meters (we experimentally verified measuring the same location different days at different hours). However, relative heights measured towards a reference can be precisely measured. We performed an experiment in a four floor building where a point in the

[1] Defined according to the International Standard Atmosphere (ISA)

roof and in the parking lot outside was measured with a RTK-GPS (Trimble 5700) with a precision of 2 *cm*. The measured height difference was of 16.23 *m*. Then the height difference was measured with the barometer 20 times within 15 minutes. The average difference was of 0.49 *m*.

IV. Localization Approach

An extended Kalman Filter (EKF) [15], [16] was used for vehicle 6 DoF localization and sensor fusion (Figure 2). The equations of the EKF are standard and on this paper only the prediction and update sensor models are detailed.

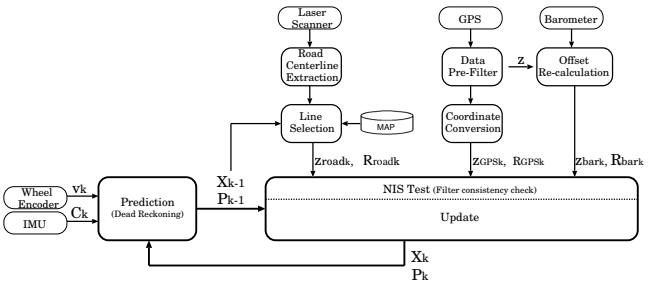

Fig. 2: Block diagram showing the vehicle localization framework. The prediction step of the EKF is computed using the wheel encoder and IMU. The update step involves map matching, GPS and barometer observations.

A. Prediction Step: Dead Reckoning

This section presents the model for a vehicle equipped with an encoder and a IMU offering 3D posture. First, the vehicle pose is given by the state vector:

$$\mathbf{x} = [x, y, z, \psi, \theta, \phi]^T, \tag{2}$$

where ψ is the yaw angle, θ is the pitch angle and ϕ is the roll angle. To avoid magnetic field disturbances [17], yaw angle is simply measured using only the yaw angular velocity ω_ψ from the IMU: $\psi = \omega_\psi \Delta t$. Pitch and roll angles are taken as computed from the IMU. Δt is the sampling time, 5*ms* for our implementation.

The posture is given by a matrix resulting from rotations in yaw, pitch and roll angles $C_k(\psi_k, \theta_k, \phi_k)$. The vehicle velocity v_k in a sample time k is measured by the wheel encoder. Then the position is given by:

$$q_k = \begin{pmatrix} x_{k-1} \\ y_{k-1} \\ z_{k-1} \end{pmatrix} + C_k(\psi_k, \theta_k, \phi_k) \begin{pmatrix} 1 \\ 0 \\ 0 \end{pmatrix} v_k \Delta t. \tag{3}$$

The predicted state is given by:

$$\mathbf{x}_{k|k-1} = f(\mathbf{x}_{k-1|k-1}, v_k, \theta_k, \Delta t) =$$

$$\begin{pmatrix} x_{k-1|k-1} + c\psi_k c\theta_k v_k \Delta t \\ y_{k-1|k-1} + s\psi_k c\theta_k v_k \Delta t \\ z_{k-1|k-1} - s\theta_k v_k \Delta t \\ \psi_{k-1|k-1} + \omega_{\psi_k k} \Delta t \\ \theta_k \\ \phi_k \end{pmatrix}. \tag{4}$$

The Jacobian matrix of the model for the predicted covariance is given by:

$$F_k = \begin{pmatrix} 1 & 0 & 0 & -s\psi_k c\theta_k v_k \Delta t & -s\theta_k c\psi_k v_k \Delta t & 0 \\ 0 & 1 & 0 & c\psi_k c\theta_k v_k \Delta t & -s\theta_k s\psi_k v_k \Delta t & 0 \\ 0 & 0 & 1 & 0 & -c\theta_k v_k \Delta t & 0 \\ 0 & 0 & 0 & 1 & 0 & 0 \\ 0 & 0 & 0 & 0 & 1 & 0 \\ 0 & 0 & 0 & 0 & 0 & 1 \end{pmatrix}. \tag{5}$$

B. Update Step

Measurement models for road centerline, GPS and barometer corrections are explained in the following subsections. These corrections update the predicted state of the filter in different sample times and are independent of each other.

1) Position Correction Using Road Centerline: A digital map available from the Japanese Geographical Survey Institute (commercially available) was used for lateral displacement correction. The map corresponds to the Kanto Region of Japan and has a $1:2500$ scale containing the road centerline network of the selected region. Using GIS tools, (ArcGIS ver 9.2) the map was transformed to Japanese Geodetic Datum 2000 (JGD 2000) Cartesian plane region *IX* [18]. The map is defined by a set of consecutive waypoints which are placed in inflexion points of the road. Consecutive waypoints were unified by straight lines. Each straight line i is defined by two parameters, the perpendicular distance from the origin to the centerline ρ_i and the angle of that perpendicular line γ_i. The vehicle's position is corrected using the perpendicular distance from its estimated position to the centerline. The experimental path is a two-way road, so the vehicle does not run always on the center. In order to compute the distance of the vehicle towards the road, the tilted lidar is used to extract the road. Road extraction is out of the scope of this paper a detailed reference of the method utilized can be found in [19]. The vehicle's position is corrected using the perpendicular distance from its estimated position towards the extracted to the centerline and compared with the map. The observation at a time k is given as:

$$\mathbf{z}_{road_k} = \frac{a x_{k|k-1} + b y_{k|k-1} + c}{\sqrt{a^2 + b^2}}, \tag{6}$$

and the variance is: $R_{road_k} = \sigma^2_{\rho\rho_k}$ which is the variance of the extracted road centerline points detected with the lidar. For a time k using the i^{th} road centerline, the observation model is:

$$\mathbf{h}_{road}(\mathbf{x}_{k|k-1,i}) = \rho_i - (x_{k|k-1}\cos(\gamma_i) + y_{k|k-1}\sin(\gamma_i)), \tag{7}$$

The Jacobian matrix of the observation model is:

$$H_{road_k} = \begin{pmatrix} -cos(\gamma_i) & -sin(\gamma_i) & 0 & 0 & 0 & 0. \end{pmatrix}. \tag{8}$$

A detailed explanation for line landmark extraction and observation models see [20] and [21]. There must be correspondence between the predicted and the observed road centerlines. To select the correct road centerline from the map to correct the vehicle position, if the vehicle enters

a rectangle area of the length of the line between two consecutive waypoints and a width of $10m$ and the estimated yaw angle $\psi_{k|k-1}$ is within $\pm 10^o$ of the angle of the line α_i ($\alpha_i = \gamma_i + 90^o$), then the line segment is selected and used to correct the vehicle lateral position.

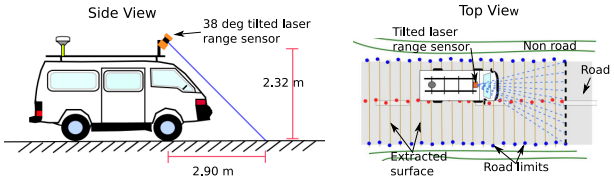

(a) Side and top views of the van car.

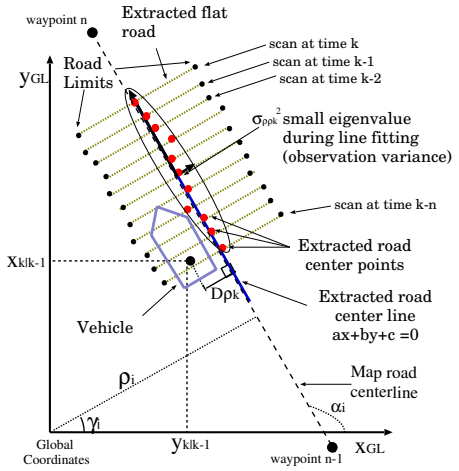

(b) Road centerline extraction.

Fig. 3: Van car vehicle and road centerline extraction with tilted lidar.

2) GPS position measurement model: The DGPS receiver outputs on-line text sentences in NMEA 0183 format. NMEA sentence GGA provides latitude, longitude, height and a $2D$ or $3D$ data type index. Coordinate conversion is performed to transform latitude and longitude from WGS84 to JGD 2000 coordinate system. Ellipsoidal height is used as measured from GPS. Observation vector is given by $\mathbf{z}_{GPS_{2D}} = [x,y]^T$ and $\mathbf{z}_{GPS_{3D}} = [x,y,z]^T$ for $2D$ and $3D$ respectively. GST sentence (Pseudorange noise statistics) for measurement standard deviation information. Standard deviation information is used to calculate covariance matrix of GPS observation in $2D$ and $3D$ given by $R_{GPS_{2D}} = \begin{pmatrix} \sigma_{xx}^2 & \sigma_{xy}^2 \\ \sigma_{yx}^2 & \sigma_{yy}^2 \end{pmatrix}$ and $R_{GPS_{3D}} = \begin{pmatrix} \sigma_{xx}^2 & \sigma_{xy}^2 & 0 \\ \sigma_{yx}^2 & \sigma_{yy}^2 & 0 \\ 0 & 0 & \sigma_{zz}^2 \end{pmatrix}$ respectively, as GPS does not provide information about the correlation between x and y with z, then σ_{xz} and σ_{yz} are considered zero (uncorrelated). The observation model is given by $\mathbf{h}_{GPS_{2D}}(\mathbf{x}_{k|k-1}) = \begin{bmatrix} x & y \end{bmatrix}^T$ and $\mathbf{h}_{GPS_{3D}}(\mathbf{x}_{k|k-1}) = \begin{bmatrix} x & y & z \end{bmatrix}^T$. Finally the Jacobian matrix is $H_{GPS_{2D}} = \begin{pmatrix} 1 & 0 & 0 & 0 & 0 & 0 \\ 0 & 1 & 0 & 0 & 0 & 0 \end{pmatrix}$ and $H_{GPS_{3D}} = \begin{pmatrix} 1 & 0 & 0 & 0 & 0 & 0 \\ 0 & 1 & 0 & 0 & 0 & 0 \\ 0 & 0 & 1 & 0 & 0 & 0 \end{pmatrix}$.

Only GPS data with a value under 4 for DOP and a number of 5 or more satellites were used for position correction [22]. Data that does not satisfy this condition is highly probable to be an outlier and is discarded.

3) Barometer height measurement model : In open sky areas, when there are enough satellites in sight (4 or more), GPS receivers can measure height. However, in woodland and mountainous paths, this condition is not satisfied all the time. To cover the lack of GPS, a barometer is used. The barometer is used to measure relative height towards an offset (see section III). The approach taken in this work was to use the last available height measurement taken from GPS $3D$ data as an offset. Then the relative height towards that offset is measured by the barometer $GPS_{Last_z} = z_{bar_k} - offset$. The height observation is:

$$\mathbf{z}_{bar} = z_{bar_k} - offset. \tag{9}$$

The offset is reset when GPS is available again. the variance for barometer height is: $R_{bar_k} = \sigma_{zz_k}^2$, where σ_{zz_k} was experimentally calculated. The observation model is given by:

$$\mathbf{h}_{bar}(\mathbf{x}_{k|k-1}) = z_{k|k-1}, \tag{10}$$

and finally the Jacobian matrix of the observation model is:

$$H_{bar_k} = \begin{pmatrix} 0 & 0 & 1 & 0 & 0 & 0 \end{pmatrix}. \tag{11}$$

In Japan orthonometric [2] or mean sea level (MSL) height is used. Therefore, in this work mean sea level height is measured.

A normalized squared innovation test was used as threshold for observations outlier rejection. If the value of χ^2 is inside 95% confidence level, then the measurement update is performed, if not then observation z_k is discarded [24].

V. Experiments

A. Experimental Environment

Experiments were performed in a mountainous woodland environment, in the Mount of Tsukuba in Japan. The experimental road path had a total length of 13326.6 m and a height difference from bottom to the top of 389.3 m (heights were measured by DGPS). The authors selected three base points (A, B and C in Figure 4, which are parking lots beside the street) free of trees and cars where the vehicle could be stopped for some minutes for sensor initialization. The path followed by the vehicle is shown in a picture taken from Google Earth in Figure 4. Point A which is the start and goal point at a height of 29.6 m, point B at a height of 176.5 m and point C which is the top point at a height of 419.0 m. A total of four routes were defined. Route 1 is the path between points A and B with a length of 3223.6 m. Route 2

[2]Relationship between ellipsoidal (h), orthonometric (H) and geoidal (N) heights [23] is given by: $h = H + N$.

is the path between points B and C with a length of 3931.9 m. Route 3 is the path between points C and B with a length of 3251.0 m (different road from route 2). Finally Route 4 is the path between points B and A with a length of 2920.1 m (different from route 1).

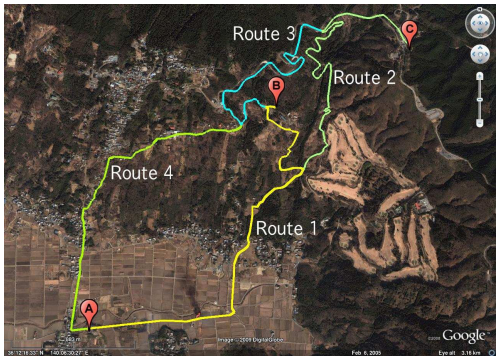

Fig. 4: Experimental path showing the base points A,B and C interconnected by routes 1,2,3 and 4. Light color show rice field areas and dark color show areas with tree foliage. Image taken from Google Earth

Roads around point A, such as lower parts of Route 1 and 4 are surrounded by rice fields shown in Figure 5a. However the rest of the roads are mainly surrounded by trees and partially covered by the mountain itself as shown in the rest pictures of Figure 5.

(a) Open sky (rice fields). (b) Dense tree foliage.

(c) Forested path. (d) Widest road section.

Fig. 5: Typical scenes of the mountainous forested path.

B. Experimental Procedure

First the sensors were initialized at the goal point A, then at each base point vehicle stopped some minutes for GPS re-initialization. Experiment start position was selected to be a tree free environment where DGPS could be initialized at point A. Then we manually drove the vehicle at a maximum speed of 40 km/h (11.1 m/sec) to the point B through Route 1, and the point C following Route 2. Finally we drove down to point B through Route 3 and to the goal point A following Route 4.

C. Experimental Results

The performance of vehicle position correction using only the road centerline is shown in Figure 6.

$2D$ estimation results using road centerline, DGPS and barometer corrections of the whole experimental path showing the original centerline map and the estimated position with its correspondent error ellipses (2σ) are illustrated in Figure 6a. Enlarged sections of 6a are shown in Figures 6b, 6c, 6d and 6e.

Figure 7 illustrates the estimated height *vs*. the travelled distance through all the routes. Through routes 1 and 4 DGPS (in dark points) was available most of the path where there were only brief barometer corrections (in light points). In routes 2 and 3 DGPS was barely available, though, properly covered by the barometer. This shows the complementary functionality of the proposed DGPS-Barometer framework to correct dead reckoning for vehicle $3D$ position estimation.

D. Extension to 3DRoad Centerline Map

$3D$ road centerline maps are built adding the estimated height to the available map. Estimated height and width is added to each waypoint of the original map as the vehicle traversed through. Road width is computed based on the lidar data of the road sides using a weighted moving average filter taking into consideration the road width average of the last 5 computed values. Additional waypoints are added only if there is a height change bigger than 1.5 m (this number was selected taking into account the precision of the barometer of 1.2 m) between the previous waypoint and the actual position of the vehicle. Each new waypoint is added in the projection of the vehicle actual position to the road centerline map. The resulting map is shown in Figure 8. As waypoints were added to the new extended map, the final map had an increment of 11.5% of waypoints (from 1214 in the original map to 1354 in the extended map).

E. Discussion

Compared towards map matching approaches that assume that the vehicle is always on the road, in our approach, the correction model only decreases uncertainty perpendicular to the road (as it actually happens). If the vehicle runs away from the road, then estimation using GPS and dead reckoning is still feasible. The $3D$ dead reckoning approach presented in this work offers a precision of 5% in curved roads and within 3% in straight roads. The estimated position in 2D offered a precision within $3m$. The drawbacks of the system are: during lack of DGPS, the system relies on the accuracy and precision of a previously available map for correcting its $2D$ position. In the case of heavy traffic the road centerline would probably not be extracted. Though dead reckoning and DGPS could still correct the vehicle position. The barometer was used for measuring height changes towards an offset taken from a fixed DGPS measurement which is assumed non-biased, therefore, the height correction inherits the offset

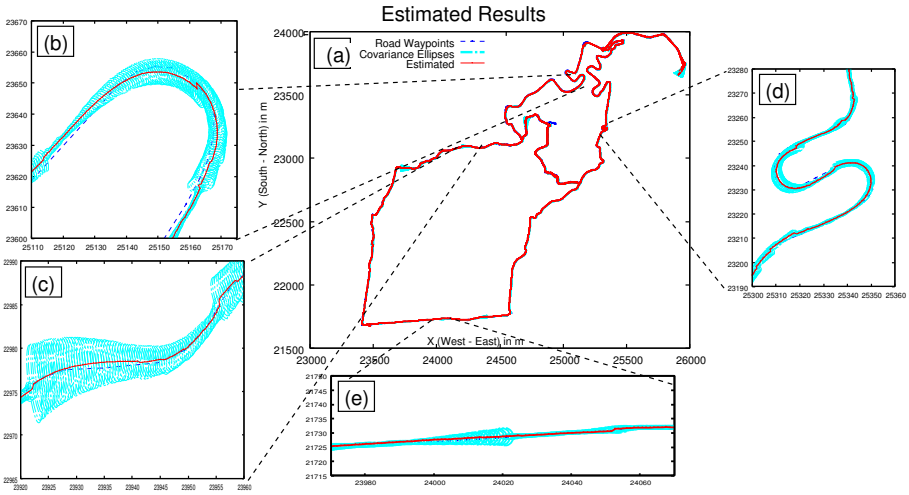

Fig. 6: Estimated position results of the whole course in (a). The error ellipses represent 2σ. (b), (c), (d) and (e) show enlarged sections of the experimental path where dead reckoning was corrected by the road centerline and DGPS-Barometer.

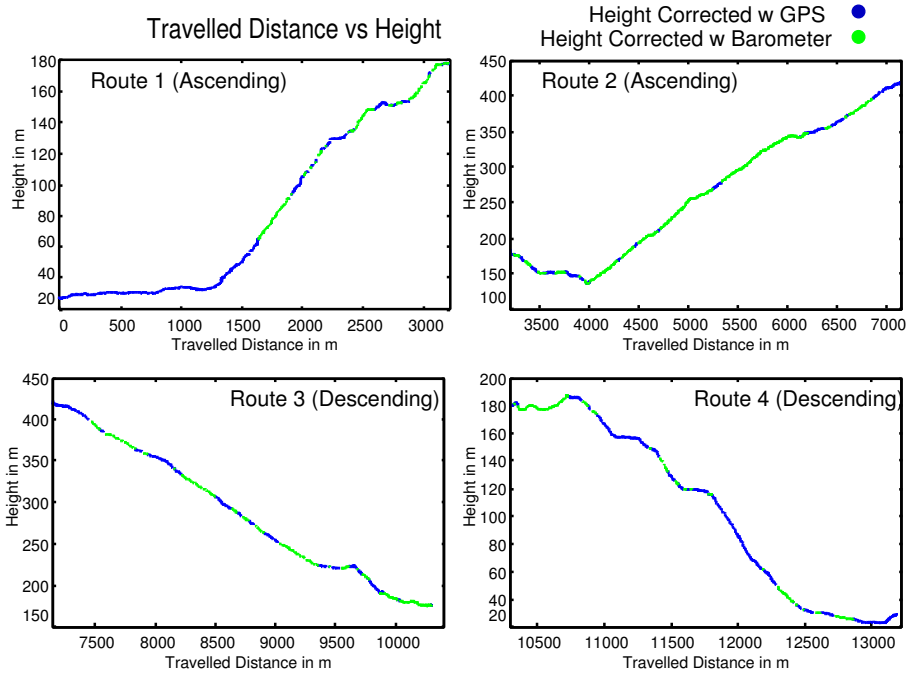

Fig. 7: Height *vs*. travelled distance estimated results. The graphs show the estimated height when an observation was available. The GPS (dark) and barometer (light) corrections are illustrated in different coloring.

error. An approach to avoid this issue is the use of two identical barometers, placing one of them as a reference with a known height sending the offset to the other one located in the rover measuring the change in height.

VI. CONCLUSIONS

In this paper, a $6DoF$ localization method for a vehicle traversing in mountainous woodland paths was detailed. The approach for using road centerline for vehicle position correction was explained. Moreover, the use of a barometer sensor for height correction during GPS blackouts was proposed. Finally, the method to extend a $2D$ road centerline map to a $3D$ map containing the centerline, the width, and the height was explained. As future work the authors plan to develop an approach where with only the vehicle height known and a $3D$ road map available, hypotheses of the vehicle location within the map can be created to achieve global localization. Furthermore, the performance of GPS height measurements in mountainous environments have to be investigated.

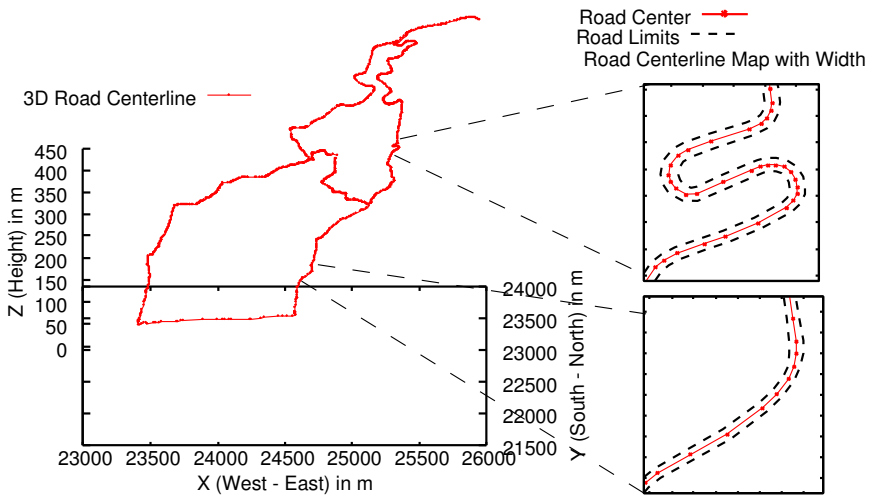

Fig. 8: Road centerline waypoints with height information in the top and width information in the bottom.

REFERENCES

[1] J. Guivant, E. Nebot, and S. Baiker, "Autonomous navigation and map building using laser range sensors in outdoor applications," *Journal of Robotic Systems*, vol. 17, pp. 3817–3822, 2000.

[2] J. Guivant, F. Masson, and E. Nebot, "Simultaneous localization and map building using natural features and absolute information," *Robotics and Autonomous Systems*, vol. 40, pp. 79–90(12), 31 August 2002.

[3] J. Jutila, K. Kannas, and A. Visala, "Tree measurement in forest by 2d laser scanning," in *Proceedings of the International Symposium on Computational Intelligence in Robotics and Automation 2007*, 2007, pp. 491–496, international Symposium on Computational Intelligence in Robotics and Automation, Jacksonville USA April 2007.

[4] M. Miettinen, M. Ohman, A. Visala, and P. Forsman, "Simultaneous localization and mapping for forest harvesters," in *Proceedings of the IEEE International Conference on Robotics and Automation 2007*, 2007, pp. 517–522, iEEE International Conference on Robotics and Automation, Rooma April 2007.

[5] P. Forsman and A. Halme, "3-d mapping of natural environments with trees by means of mobile perception," *IEEE Transactions on Robotics*, vol. 21, no. 3, pp. 482–490, 2005.

[6] K. Kodagoda, C.-C. Wang, and G. Dissanayake, "Laser based sensing on roads," in *Proc. of the Intelligent Vehicles and Road Infrastructure Conf.*, Melbourne, Australia, 2005.

[7] R. Kümmerle, R. Triebel, P. Pfaff, and W. Burgard, "Monte carlo localization in outdoor terrains using multilevel surface maps," *Journal of Field Robotics*, vol. 25, no. 6-7, pp. 346–359, 2008.

[8] M. E. E. Najjar and P. Bonnifait, "A road-matching method for precise vehicle localization using belief theory and kalman filtering," *Autonomous Robots*, vol. 19, no. 2, pp. 173–191, September 2005.

[9] C. Urmson, J. Anhalt, H. Bae, J. D. Bagnell, C. Baker, R. E. Bittner, T. Brown, M. N. Clark, M. Darms, D. Demitrish, J. Dolan, D. Duggins, D. Ferguson, T. Galatali, C. M. Geyer, M. Gittleman, S. Harbaugh, M. Hebert, T. Howard, S. Kolski, M. Likhachev, B. Litkouhi, A. Kelly, M. McNaughton, N. Miller, J. Nickolaou, K. Peterson, B. Pilnick, R. Rajkumar, P. Rybski, V. Sadekar, B. Salesky, Y.-W. Seo, S. Singh, J. M. Snider, J. C. Struble, A. T. Stentz, M. Taylor, W. R. L. Whittaker, Z. Wolkowicki, W. Zhang, and J. Ziglar, *Autonomous driving in urban environments: Boss and the Urban Challenge*, vol. 25, no. 1, pp. 425–466, June 2008.

[10] M. Montemerlo, J. Becker, S. Bhat, H. Dahlkamp, D. Dolgov, S. Ettinger, D. Haehnel, T. Hilden, G. Hoffmann, B. Huhnke, D. Johnston, S. Klumpp, D. Langer, A. Levandowski, J. Levinson, J. Marcil, D. Orenstein, J. Paefgen, I. Penny, A. Petrovskaya, M. Pflueger, G. Stanek, D. Stavens, A. Vogt, and S. Thrun, *Journal of Field Robotics Special Issue on the 2007 DARPA Urban Challenge, Part II*, vol. 25, no. 1, pp. 569–597, September 2008.

[11] A. Bacha, C. Bauman, R. Faruque, M. Fleming, C. Terwelp, C. Reinholtz, D. Hong, A. Wicks, T. Alberi, D. Anderson, , S. Cacciola, P. Currier, , A. Dalton, J. Farmer, J. Hurdus, S. Kimmel, P. King, A. Taylor, D. V. Covern, and M. Webster, *Team VictorTango's entry in the DARPA Urban Challenge*, vol. 25, no. 1, pp. 467–492, June 2008.

[12] J. Bohren, T. Foote, J. Keller, A. Kushleyev, D. Lee, A. Stewart, P. Vernaza, J. Derenick, J. Spletzer, and B. Satterfield, *The Ben Franklin Racing Team's entry in the 2007 DARPA Urban Challenge*, vol. 25, no. 1, pp. 598–614, September 2008.

[13] J. Leonard, J. How, S. Teller, M. Berger, S. Campbell, G. Fiore, L. Fletcher, E. Frazzoli, A. Huang, S. Karaman, O. Koch, Y. Kuwata, D. Moore, E. Olson, S. Peters, J. Teo, R. Truax, M. Walter, D. Barrett, A. Epstein, K. Maheloni, K. Moyer, T. Jones, R. Buckley, M. Antone, R. Galejs, S. Krishnamurthy, and J. Williams, *A perception-driven autonomous urban vehicle*, vol. 25, no. 1, pp. 727–774, October 2008.

[14] I. Miller, M. Campbell, D. Huttenlocher, F.-R. Kline, A. Nathan, S. Lupashin, J. Catlin, B. Schimpf, P. Moran, N. Zych, E. Garcia, M. Kurdziel, and H. Fujishima, *Team Cornell's Skynet: Robust perception and planning in an urban environment*, vol. 25, no. 1, pp. 493–527, June 2008.

[15] R. E. Kalman, "A new approach to linear filtering and prediction problems," *Transaction of the ASME Journal of Basic Engineering*, pp. 35–45, March 1960.

[16] P. S. Maybeck, *Stochastic models, estimation, and control*, ser. Mathematics in Science and Engineering. Academic Press, 1979, vol. 1.

[17] E. R. Bachmann, X. Yun, and C. W. Peterson, "An investigation of the effects of magnetic variations on inertial magnetic orientation sensors," *IEEE Robotics and Automation Magazine*, pp. 76–87, September 2007.

[18] Geographical, "Geographical survey institute government of japan [www page]." Retrieved August 2, 2008 from http://vldb.gsi.go.jp/sokuchi/surveycalc/, 2008.

[19] Y. Morales, E. Takeuchi, A. Carballo, A. Aburadani, and T. Tsubouchi, "Autonomous robot navigation in outdoor cluttered pedestrian walkways (submitted)," *Journal of Field Robotics*.

[20] K. O. Arras and Y. Siegwart, "Feature extraction and scene interpretation for map-based navigation and map building," in *In Proceedings of SPIE, Mobile Robotics XII*, 1997, pp. 42–53.

[21] R. Siegwart and I. Nourbakhsh, *Introduction to Autonomous Mobile Robots*, 2004, a Bradford Book, The MIT Press, Cambridge, Massachusetts, London, England. [Online]. Available: http://www.mobilerobots.org

[22] Y. Morales and T. Tsubouchi, "Gps moving performance on open sky and forested paths," in *Proceedings of the 2007 IEEE/RSJ International Conference on Intelligent Robots and Systems (IROS)*, San Diego Ca, October 2007, pp. 3180–3185.

[23] B. Hofmann-Wellenhof, H. Lichtenegger, and J. Collins, *GPS: Theory and Practice (Fifth Revised Edition)*. Springler-Verlag Wien, December 2001.

[24] X. L. Y Bar-Shalom and T. Kirubarajan, *Estimation with Applications ot Tracking and Navigation*. Wiley-Interscience Publication, 2001.